

Al₂O₃-C_{act} Derivatives: Synthesis and Properties

Edita KIRPŠAITĖ*, Gitana DABRILAITĖ-KUDŽMIENĖ, Saulius KITRYS

Faculty of Chemical Technology, Kaunas University of Technology, Radvilėnų pl. 19, LT-50254 Kaunas, Lithuania

Received 02 July 2010; accepted 27 October 2010

In the present work Al₂O₃-C_{act} binary derivatives were synthesized by sol-gel method. Thermal resistance of these derivatives is 70 °C–200 °C higher (depending on activated carbon type) compared to pure carbons. For the analysis of these composites X-ray diffraction (XRD) and infrared spectroscopy (IR) were used.

The adsorption of acetone and water vapor as well as thermal regeneration at 100 °C of wet samples was investigated. Results show that Al₂O₃-C_{act} derivatives are hydrophobic: water vapor is adsorbed slowly; calculated low values of adsorption coefficient show weak interaction between adsorbent and adsorbate. Acetone vapor adsorption is fast, equilibrium is reached in 80 min–120 min. Water vapor from the wet Al₂O₃-C_{act} surface is eliminated in ~70 min at 100 °C.

Keywords: sol-gel synthesis, composite adsorbents; alumina gel; activated carbon, thermal stability, adsorption.

INTRODUCTION

Activated carbons are used as adsorbents and catalyst carriers. Currently, activated carbon production capacity worldwide is about 1 million tons per year and is constantly growing due to its emerging traditional and modern applications [1]. In practice, activated carbons are used in many fields: about 40 % of activated carbon in the world is used in the food industry, 30 % in respiratory protection systems (respirators, gas masks, etc.), 15 % for water purification, 5 % in medicine [2]. The use for adsorption processes is determined by large specific surface area (up to 3000 m²/g) [3–6]. About 1 % of total activated carbon production volume is used for the production of catalysts [7]. Activated carbons consist of neutral C atoms so they adsorb both polar and non-polar adsorbate molecules. They are hydrophobic and primarily adsorb hydrophobic materials such as organic solvents. Activated carbons are non-selective and are suitable for use at wet pre-adsorption gas streams for both inorganic and volatile organic compounds (VOC) adsorption cases [8].

The application of activated carbons is limited by their low thermal resistance and the conditions of thermal regeneration. In oxidizing environment (O₂, air, water vapor, etc.) carbon reaction with oxygen or oxygen radicals begins above 200 °C. It is known that [9] the thermal stability of such adsorbents can be increased by coupling them with thermo stable additives (SiO₂, Al₂O₃, TiO₂, etc.). Such binary adsorbents present different characteristics than primary components [10, 11]. In [12] binary Al₂O₃-C_{act} derivatives containing ~5 % of the WS-42A type activated carbon were investigated. The thermal resistance of such composites is higher by more than 50 °C as compared to pure activated carbon.

Al₂O₃-C_{act} derivatives are used for the preparation of electrochemical sensors [13, 14], in metallurgy [15], as catalyst support [16], for water treatment [17], high performance liquid chromatography [18], etc.

However, there is a lack of information about the application for gas purification. Some information about activated carbon and porous alumina gel derivatives can be found in Neimark's works [19].

The aim of this work was to synthesize thermo stable wide-pores alumina gel and close-pores activated carbon composite materials and to determine their adsorptive properties. The derivatives were tested as adsorbents for water and acetone vapor. Activated carbons chosen for the synthesis of adsorbents are used in industry for acetone vapor removal [20].

MATERIALS AND EXPERIMENTAL METHODS

The activated carbons used in the present work were WS-42 (Chemviron Carbon, Germany), B-2 (Norit, Netherlands) and OU (Ukraine), granulated up to 50 μm fraction [12]. For the synthesis of Al₂O₃-C_{act} composites the sol-gel method was used by adding the activated carbon into 1 M Al₂(SO₄)₃ solution, later 1 M NaOH by portions. Wet alumina gel-activated carbon derivatives were granulated by extrusion (granules 1.2 mm–1.5 mm in diameter), then dried at 120 °C for 4 h and heated at 420 °C for 4 h. The amount of activated carbon in the adsorbents was ~5 % (wt).

Mineral composition of the prepared adsorbents was examined by X-ray diffraction (XRD) analysis using "DRON-6" diffractometer (CuK_α radiation, nickel filter, detector movement step 0.02°, measurement time step 0.5 s, voltage $U = 30$ kV, current $I = 20$ mA).

IR spectra analysis was performed using "Perkin Elmer FT-IR System" spectrometer in infrared spectrum region from 4000 cm⁻¹ to 400 cm⁻¹.

Differential scanning calorimetry-thermogravimetry (DSC-TG) was performed with a "Netzsch STA 409 PC Luxx" (Germany) calorimeter. DSC-TG analysis parameters: temperature range 30 °C–800 °C, heating rate 15 °C/min, standart – empty Pt/Rh crucible, atmosphere in the furnace – air, mass of studied sample 30 mg–34 mg for composite materials and 5 mg–7 mg for activated carbon.

*Corresponding author. Tel.: +370-37-300169, fax.: +370-37-300152.
E-mail address: edita.kirpsaite@gmail.com (E. Kirpšaitė)

The thermal resistance of granular composite adsorbents was determined by heating the samples in a furnace with air environment and measuring the weight change by increasing the heating temperature. The samples were heated at each temperature for about 1 hour. Step of temperature rise was 50 °C.

The adsorption capacity was measured by an experimental set-up described in detail in [12]. Briefly, it consists of blocks of gas mixture preparation, flow rate regulation, measurement systems and thermostated adsorption cell with the balances.

RESULTS AND DISCUSSIONS

The thermal resistance of activated carbons used for synthesis was determined using DSC-TG analysis [21] (Fig. 1). During activated carbon oxidation the exothermic effect and weight loss are obtained [22]. The results showed that WS-42A type activated carbon is thermostable up to ~420 °C, the oxidation of B-2 starts at ~300 °C, OU at ~350 °C and WS-42 already at ~250 °C. The endothermic effect obtained at ~100 °C refers to adsorbed water elimination.

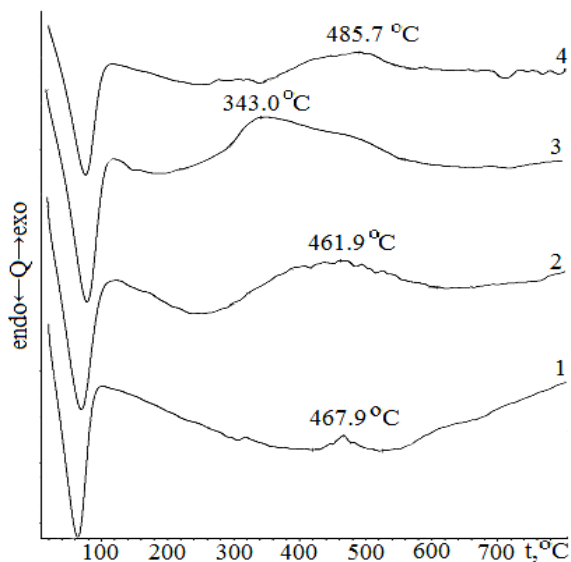


Fig. 1. DSC curves of activated carbons at air atmosphere: 1 – WS-42A, 2 – B-2, 3 – WS-42, 4 – OU

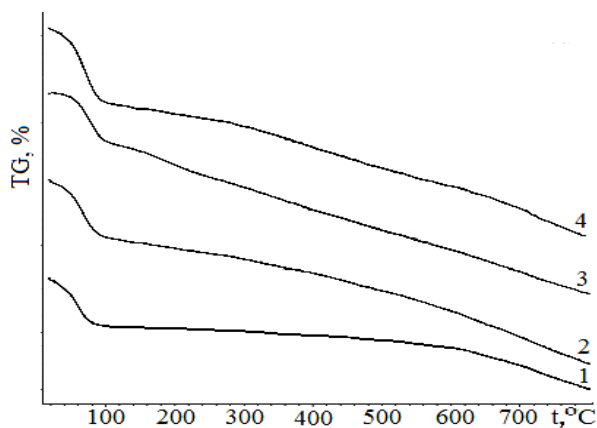


Fig. 2. TG curves of activated carbons at air atmosphere: 1 – WS-42A, 2 – B-2, 3 – WS-42, 4 – OU

The first sharp weight loss at ~100 °C in TG analysis curves (Fig. 2) is obtained due to adsorbed water elimination. Further (above 200 °C) weight loss shows the oxidation of activated carbons.

Differential scanning calorimetry was also used to determine thermal stability of prepared wet $\text{Al}_2\text{O}_3\text{-C}_{\text{act}}$ composite materials (Fig. 3). The criteria of thermal stability is the oxidation start temperature. Slight endothermic effects at 100 °C–140 °C at air atmosphere are obtained due to the desorption of water. Exothermic effects beginning at 450 °C refer to carbon oxidation. Data show that the most thermally resistant is the adsorbent $\text{Al}_2\text{O}_3\text{-C}_{\text{act}}$ with WS-42A type activated carbon (Fig. 3, curve 1). The oxidation starts at ~500 °C. Similarly, the composite adsorbent with B-2 activated carbon is heat resistant up to ~460 °C, with OU and WS-42 activated carbons up to ~450 °C.

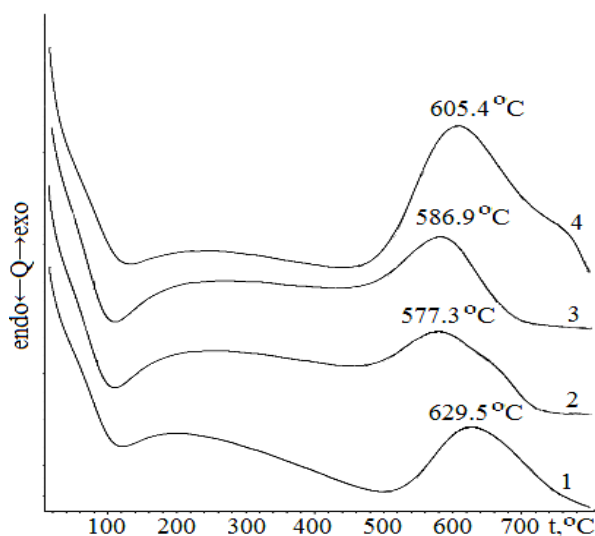


Fig. 3. DSC curves of $\text{Al}_2\text{O}_3\text{-C}_{\text{act}}$ at air atmosphere: 1 – $\text{Al}_2\text{O}_3\text{-(WS-42A)}$, 2 – $\text{Al}_2\text{O}_3\text{-(B-2)}$, 3 – $\text{Al}_2\text{O}_3\text{-(WS-42)}$, 4 – $\text{Al}_2\text{O}_3\text{-(OU)}$

Weight loss in TG curves (Fig. 4) starting at 100 °C can be attributed to water elimination from wet derivatives. While dehydration process still proceeds, above 450 °C the oxidation of activated carbons occurs.

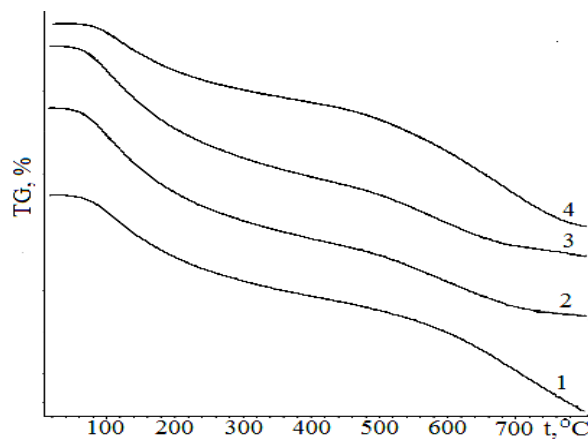


Fig. 4. TG curves of $\text{Al}_2\text{O}_3\text{-C}_{\text{act}}$ at air atmosphere: 1 – $\text{Al}_2\text{O}_3\text{-(WS-42A)}$, 2 – $\text{Al}_2\text{O}_3\text{-(B-2)}$, 3 – $\text{Al}_2\text{O}_3\text{-(WS-42)}$, 4 – $\text{Al}_2\text{O}_3\text{-(OU)}$

Results of TG analysis for various synthesized mesoporous alumina samples have been reported [23]. Sun at al. analyzed prepared alumina by TG method. The weight loss of the samples proceeded until 600 °C due to dehydration. Above this temperature the weight loss process was stabilized indicating the beginning of various alumina phase transformations.

Additionally, thermal analysis used for activated carbons and $\text{Al}_2\text{O}_3\text{-C}_{\text{act}}$ derivatives show that alumina gel coating in synthesized composites increases thermal stability of activated carbons. Yilmaz at al. [15] synthesized boehmite alumina coated graphite by sol-gel method covering graphite by the alumina layer. Their produced composite was not more thermostable than graphite used for synthesis. The oxidation start temperature for both samples was ~650 °C. In this case alumina coating just increased the oxidation interval of carbon.

Thermal resistance of composites was also studied using thermogravimetry analysis by heating samples at various temperatures (Table 1).

While heating wet granular composite adsorbents at temperatures of 100 °C–300 °C the differential weight changes are obtained. They can be attributed to water evaporation. The weight loss of adsorbents at 400 °C–550 °C is related to activated carbon oxidation with air oxygen. The oxidation of activated carbons starts respectively: for WS-42A at ~500 °C, for B2, OU and WS-42 at ~450 °C.

The XRD patterns (Fig. 5) show that amorphous structure with crystalline particles dominates in the $\text{Al}_2\text{O}_3\text{-C}_{\text{act}}$ composite materials. The peaks are characteristic to activated carbon, $\gamma\text{Al}_2\text{O}_3$ and boehmite. Other researchers [15, 23–24] such materials with faintly expressed peaks call amorphous. The same patterns are obtained with different activated carbons which show that the structure is not carbon-type dependent.

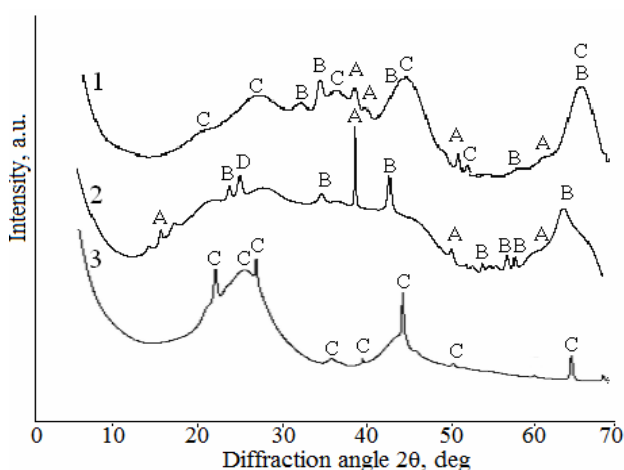


Fig. 5. X-ray diffraction patterns of: 1 – $\text{Al}_2\text{O}_3\text{-C}_{\text{act}}$ composite, 2 – Al_2O_3 , 3 – WS-42A activated carbon. A – $\text{AlO}(\text{OH})$, B – $\gamma\text{Al}_2\text{O}_3$, C – carbon, D – $\text{Al}_2(\text{SO}_4)_3$

Furthermore, this assumption is confirmed by IR analysis (Fig. 6). All curves are almost identical and their patterns do not depend on activated carbon type.

A broad absorption band at 3500 cm^{-1} (valence O–H vibrations), together with the absorption band at 1640 cm^{-1} (HOH vibrations) are characteristic for water

molecules. The peaks at $(1139\text{--}1122)\text{ cm}^{-1}$ can be attributed to the presence of free SO_4^{2-} ions and double peaks at the range of $(850\text{--}620)\text{ cm}^{-1}$ are characteristic for Al–O–Al bonds [15, 25].

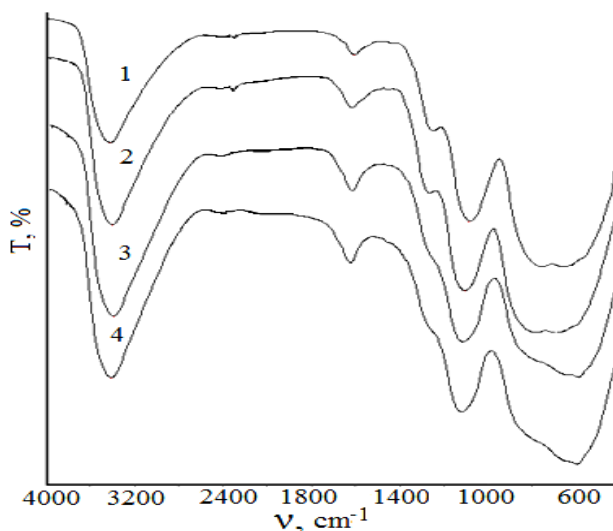


Fig. 6. IR patterns for various $\text{Al}_2\text{O}_3\text{-C}_{\text{act}}$ derivatives: 1 – $\text{Al}_2\text{O}_3\text{-(WS-42A)}$, 2 – $\text{Al}_2\text{O}_3\text{-(B-2)}$, 3 – $\text{Al}_2\text{O}_3\text{-(OU)}$, 4 – $\text{Al}_2\text{O}_3\text{-(WS-42)}$

The maximum $\text{Al}_2\text{O}_3\text{-C}_{\text{act}}$ adsorption capacity for acetone vapor was measured using acetone vapor concentration of $681\text{ g/cm}^3\text{--}694\text{ g/cm}^3$ in the preadsorptive air-vapor mixture (Fig. 7).

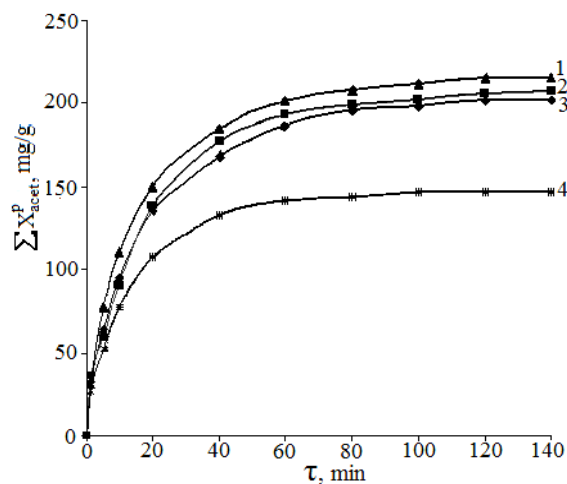


Fig. 7. Kinetic curves of acetone vapor adsorption at 22 °C, 748 mmHg–763 mmHg, air humidity 40 %–45 % for various adsorbents: 1 – $\text{Al}_2\text{O}_3\text{-(OU)}$, 2 – $\text{Al}_2\text{O}_3\text{-(B-2)}$, 3 – $\text{Al}_2\text{O}_3\text{-(WS-42A)}$, 4 – $\text{Al}_2\text{O}_3\text{-(WS-42)}$

Under these conditions acetone vapors are in equilibrium with the liquid acetone at 22 °C (partial pressure $p/p_0 \sim 1$, adsorption pressure is close to atmospheric).

It was determined that $\text{Al}_2\text{O}_3\text{-(WS-42)}$ adsorbed 146.68 mg/g of acetone vapor. Adsorption equilibrium was reached in ~80 min. Equilibrium adsorption capacity for $\text{Al}_2\text{O}_3\text{-(WS-42A)}$, $\text{Al}_2\text{O}_3\text{-(B-2)}$ and $\text{Al}_2\text{O}_3\text{-(OU)}$ adsorbents is higher and ranges between 201.47 mg/g and 215.68 mg/g. In these cases adsorption equilibrium is reached within ~100 min–120 min.

Table 1. Differential weight changes of wet $\text{Al}_2\text{O}_3\text{-C}_{\text{act}}$ samples at air atmosphere depending on temperature

$\text{Al}_2\text{O}_3\text{-C}_{\text{act}}$	Differential weight changes Δm , mg/g									
	100 °C	200 °C	250 °C	300 °C	350 °C	400 °C	450 °C	500 °C	550 °C	600 °C
WS-42A	125.75	137.54	77.45	33.95	17.08	14.11	8.36	12.73	32.75	19.68
B-2	111.79	139.43	89.94	40.41	19.28	11.16	15.68	27.83	8.82	2.76
OU	206.54	434.26	200.68	21.78	4.65	2.10	3.38	6.89	3.19	1.11
WS-42	177.90	367.80	242.75	49.42	8.08	4.40	5.40	6.28	2.87	2.28

The adsorption capacities of such activated carbons for acetone vapor are much bigger (357 mg/g–451 mg/g) compared to $\text{Al}_2\text{O}_3\text{-C}_{\text{act}}$ derivatives under identical conditions. However, the advantage of such composite materials is a higher thermal resistance which is needed in chemical industry.

After the adsorption process activated carbons saturated with acetone vapor are mostly regenerated using water vapor. Unsuitable conditions for adsorption and regeneration during adsorbents operation can reduce their adsorption capacity. Therefore, adsorption and regeneration studies of composite $\text{Al}_2\text{O}_3\text{-C}_{\text{act}}$ adsorbents are also important.

Equilibrium adsorption capacity for water vapor was measured over $\text{H}_2\text{SO}_4\text{-H}_2\text{O}$ mixture under stationary conditions. Water vapor was in equilibrium with the $\text{H}_2\text{SO}_4\text{-H}_2\text{O}$ solution at 25 °C, pressure being close to atmospheric. Different concentrations of sulfuric acid solutions were used for experiments (10 %–90 %). Under these conditions water vapor partial pressure ratio p/p_0 varied from 0.0003 to ~1 [26].

The maximum amount of water is adsorbed when pressure ratio is close to 1. In this case, adsorption is slow; the amount of adsorbed water $\sum X_{\text{H}_2\text{O}}^p$ after 3 hours is similar for all adsorbents and varies between 134.12 mg/g and 158.89 mg/g.

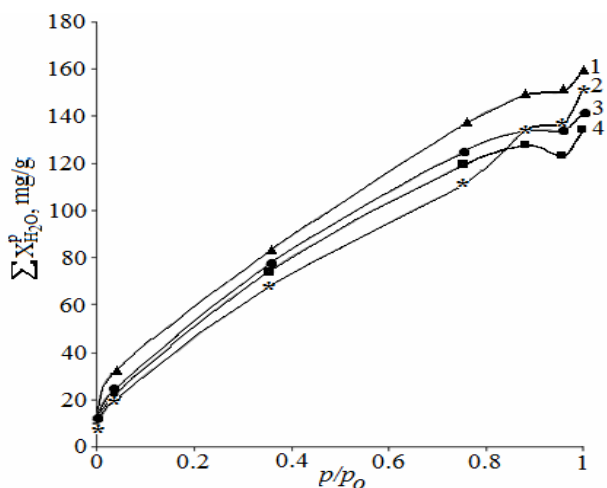


Fig. 8. Water vapor adsorption isotherms at 25 °C: 1 – $\text{Al}_2\text{O}_3\text{-(OU)}$, 2 – $\text{Al}_2\text{O}_3\text{-(WS-42A)}$, 3 – $\text{Al}_2\text{O}_3\text{-(B-2)}$, 4 – $\text{Al}_2\text{O}_3\text{-(WS-42)}$

The obtained isotherms (Fig. 8) are ascribed to be of the 4th type [27]. Such isotherms are characteristic for many industrial porous adsorbents and catalysts. Increasing

the ratio p/p_0 the capillary condensation in adsorbents pores occurs and adsorption rate is considerably increased.

Monolayer capacity and adsorption coefficient is calculated according to transformed Langmuir equation [28]:

$$\frac{p_i}{\sum X_p} = \frac{1}{X_m b} + \frac{1}{X_m} p_i,$$

where p_i is water vapor partial pressure in pre-adsorption vapor mixture, mmHg; X_m is monolayer capacity for water vapor, mg/g; b is adsorption coefficient.

This equation is appropriate for practical calculations because in almost every case linear dependence is obtained at the coordinates $((p_i / \sum X_p) - p_i)$ (Fig. 9).

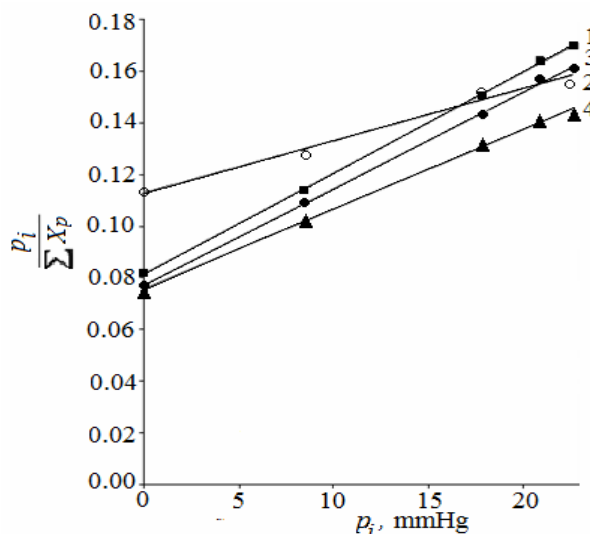


Fig. 9. Linear dependence for calculation of X_m and adsorption coefficient b : 1 – $\text{Al}_2\text{O}_3\text{-(B-2)}$, 2 – $\text{Al}_2\text{O}_3\text{-(WS-42)}$, 3 – $\text{Al}_2\text{O}_3\text{-(WS-42A)}$, 4 – $\text{Al}_2\text{O}_3\text{-(OU)}$

The calculated values of monolayer capacity X_m and adsorption coefficient b are given in Table 2. The obtained results show that monolayer capacity for studied adsorbents ranges between 263 mg/g–333 mg/g, and coefficient b is between 0.03 and 0.049.

Such low adsorption coefficient b values indicate a weak interaction between the adsorbent and adsorbate. Based on these calculations and the fact that $\text{Al}_2\text{O}_3\text{-C}_{\text{act}}$ adsorbs water vapor very slowly, it may be suggested that our produced adsorbents are hydrophobic and water vapor adsorption on $\text{Al}_2\text{O}_3\text{-C}_{\text{act}}$ surface is physical.

In order to study the regeneration of $\text{Al}_2\text{O}_3\text{-(WS-42)}$ saturated with water vapor, the granulated adsorbent was

kept in a closed vessel above water vapor ($p/p_0 \sim 1$) for 6 days. Then the composite was heated for 2 hours at 100 °C (Fig. 10).

Table 2. Langmuir equation coefficients at 25 °C

Composite	Linear equation constants		Monolayer capacity X_m , mg/g	Coefficient b
	Intercept $I = \frac{1}{X_m \cdot b}$	Slope $\text{tg} \alpha = \frac{1}{X_m}$		
Al ₂ O ₃ -(WS-42A)	0.077	0.0038	263	0.049
Al ₂ O ₃ -(B-2)	0.082	0.0037	270	0.045
Al ₂ O ₃ -(OU)	0.075	0.0031	323	0.041
Al ₂ O ₃ -(WS-42)	0.113	0.0021	333	0.030

The biggest amount of water vapor is desorbed during the first 20 min–30 min (average desorption rate is 0.97 mg/min). Under these conditions regeneration lasts about 70 min–80 min.

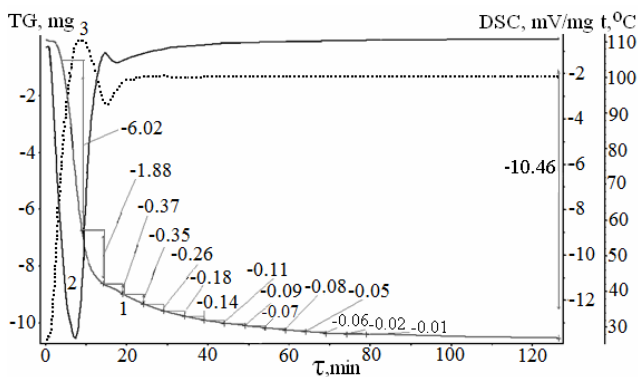


Fig. 10. Regeneration of Al₂O₃-Cact at 100 °C: 1 – TG curve, 2 – DSC curve, 3 – temperature rise curve

For the regeneration of water vapor for such materials the temperature slightly higher than 100 °C should be used to increase regeneration rate. As it is important for chemical industry that regeneration process would not last longer than 30 min. If moisture is not completely eliminated from adsorbents pores during this time, their adsorption capacity is decreasing.

CONCLUSIONS

Al₂O₃-C_{act} composite adsorbents were synthesized by sol-gel method and characterized by XRD, IR and TG-DSC analysis. It was determined that adsorbents are amorphous and more thermostable than pure activated carbons.

The maximum Al₂O₃-C_{akt} adsorption capacity for acetone vapor ($p/p_0 \approx 1$) is 146.68 mg/g–215.68 mg/g.

The adsorbent is hydrophobic and the physical adsorption of water vapor is slow. At ratio $p/p_0 \approx 1$, the adsorption capacity for all studied Al₂O₃-C_{akt} adsorbents is similar and ranges between 134.12 mg/g and 158.89 mg/g.

The calculated capacity of monomolecular water vapor layer is 263 mg/g–333 mg/g, and adsorption coefficient b is 0.03–0.049.

REFERENCES

1. **Oloncev, V. F.** Some Tendencies of Production and Application of Activated Carbons in the World *Chemical Industry* 8 2000: pp. 7–14 (in Russian).
2. **Kuznetsov, B. N.** Carbon Sorbents Synthesis and Application *Soros Educational Journal* 12 1999: pp. 29–34 (in Russian).
3. **Maldonado-Hodar, F. J., Perez-Cadenas, A. F., Morena-Castilla, C.** Morphology of Heat-treated Tungsten Doped Monolithic Carbon Aerogels *Carbon* 1 2003: pp. 1291–1299.
4. **Mattson, J., Mark, H. B., Malbin, M. D., Weber, W. J., Crittenden, J. C.** Surface Chemistry of Active Carbon: Specific Adsorption of Phenols *Journal of Colloid and Interface Science* 31 (1) 1969: pp. 116–130.
5. **Helminen, J., Helenius, J., Paatero, E., Turunen, I.** Adsorption Equilibria of Ammonia Gas on Inorganic and Organic Sorbents at 298.15 K *Journal of Chemical and Engineering Data* 46 (2) 2001: pp. 391–399.
6. **Collin, G. J., Awang, B., Duduku, K., Onn, S. K.** Sorption of Methylene Blue Dye in Aqueous Solution by Optimized Carbon Prepared from Guava Seeds (*Psidium guajava* L.) *Materials Science (Medžiagotyra)* 1 (13) 2007: pp. 83–87.
7. **Bashkova, S., Baker, F. S., Wu, X., Armstrong, T. R., Schwartz, V.** Activated Carbon Catalyst for Selective Oxidation of Hydrogen Sulphide: On the Influence of Pore Structure, Surface Characteristics, and Catalytically-active Nitrogen *Carbon* 45 (6) 2007: pp. 1354–1363.
8. **Bradley, R., Rand, B.** A Comparison of the Adsorption Behavior of Nitrogen, Alcohols and Water towards Active Carbons *Carbon* 29 (8) 1991: pp. 1165–1172.
9. **Leboda, R., Dąbrowski, A.** Chapter 1.5 Complex Carbon-mineral Adsorbents: Preparation, Surface Properties and Their Modification *Studies in Surface Science and Catalysis* 99 1996: pp. 115–146.
10. **Xingmei, G., Xuguang, L., Bingshe, X., Tao, D.** Synthesis and Characterization of Carbon Sphere-silica Core-shell Structure and Hollow Silica Spheres *Colloids and Surfaces A* 345 (1–3) 2009: pp. 141–146.
11. **Qian, X., Wan, Y., Wen, Y., Jia, N., Li, H., Zhao, D.** Synthesis of Ordered Mesoporous Crystalline Carbon-anatase Composites with High Titania Contents *Journal of Colloid and Interface Science* 328 (2) 2008: pp. 367–373.
12. **Dabrilaitė, G.** γ -Al₂O₃-C_{act}-Me_xO_y Adsorbents-catalysts: Synthesis, Properties and Practical Application *Summary of Doctoral Dissertation* Kaunas, 2005.
13. **Tsubokawa, N., Ogasawara, T., Inaba, J., Fujiki, K.** Preparation by Sol-gel Process in the Presence of Polymer-grafted Carbon Black and Its Electric Properties *Journal of Polymer Science Part A-Polymer Chemistry* 37 (18) 1999: pp. 3591–3597.
14. **Tsukubowa, N., Inaba, J., Arai, K., Fujiki, K.** Responsiveness of Electric Resistance of Polymer-grafted Carbon Black/Alumina Gel Composite against Solvent Vapor and Solute in Solution *Polymer Bulletin* 44(3) 2000: pp. 317–324.

15. **Yilmaz, S., Kutmen-Kalpakli, Y., Yilmaz, E.** Synthesis and Characterization of Boehmitic Alumina Coated Graphite by Sol-gel Method *Ceramics International* 35(5) 2009: pp. 2029–2034.
16. **Salinas-Martinez de Lecea, C., Linares-Solano, A., Diaz-Aunon, J. A., L'Argentiere, P. C.** Improvement of Activity and Sulphur Resistance of Pd Complex Catalyst Using Carbon-coated γ -Al₂O₃ and Activated Carbon Supports *Carbon* 38 2000: pp. 157–160.
17. **Leyva Ramos, R., Ovalle-Turrubiarres, J., Sanches-Castillo, M. A.** Adsorption of Fluoride from Aqueous Solution on Aluminum-impregnated Carbon *Carbon* 37 1999: pp. 609–617.
18. **Paek, C., McCormick, A. V., Carr, P. W.** Preparation and Evaluation of Carbon Coated Alumina as a High Surface Area Packing Material for High Performance Liquid Chromatography *Journal of Chromatography A* 2010: pp. 2–14.
19. **Neimark, I. E.** Synthetic Mineral Adsorbents and Catalysts Carrier. Kiev, 1982: 216 p. (in Russian).
20. **Elvers, B., Hawkins, S., Russey, W.** Ullmann's Encyclopedia of Industrial Chemistry. Vol. 45. New York, 1986: 556 p.
21. **Brown, M. E.** Introduction to Thermal analysis: Techniques and Applications. Springer, New York, 2001: 280 p.
22. **Illekova, E., Csomorova, K.** Kinetics of Oxidation in Various Forms of Carbon *Journal of Thermal Analysis and Calorimetry* 80 2005: pp. 103–108.
23. **Sun, Z.-X., Zheng, T.-T., Bo, Q.-B., Du, M., Forsling, W.** Effects of Calcination Temperature on Pore Size and Wall Crystalline Structure of Mesoporous Alumina *Journal of Colloid and Interface Science* 319 2008: pp. 247–251.
24. **Guo, X., Liu, X., Xu, B., Dou, T.** Synthesis and Characterization of Carbon Sphere-silica Core-shell Structure and Hollow Silica Spheres *Colloids and Surfaces A* 324 (1–3) 2009: pp. 141–146.
25. **Buika, G., Getautis, V., Martynaitis, V., Rutkauskas, K.** Spectroscopy of Organic Compounds. Vitae Litera, 2007: 277 p. (in Lithuanian).
26. Short Reference Book of Chemistry. Kiev, 1974: 432 p. (in Russian).
27. **Noll, K., Gounaris, V., Hou, W.** Adsorption Technology for Air and Water Pollution Control. Lewis Publishers, Michigan, 1992: 347 pp.
28. **Bartholomew, C. H., Farrauto, R. J.** Fundamentals of Industrial Catalytic Processes. Wiley and Sons, New York, 2006: 966 p.